REPORT DOCUMENTATION PAGE

Form Approved
OMB No. 0704-01-0188

1. REPORT DATE *(DD-MM-YYYY)*
11-01-2007

2. REPORT TYPE
REPRINT

3. DATES COVERED *(From - To)*

4. TITLE AND SUBTITLE
Nascap-2k Spacecraft-Plasma Environment Interactions Modeling: New Capabilities and Verification

5a. CONTRACT NUMBER

5b. GRANT NUMBER

5c. PROGRAM ELEMENT NUMBER
61102F

6. AUTHORS
V.A. Davis*, M.J. Mandell, D.L. Cooke, and D.C. Ferguson**

5d. PROJECT NUMBER
1010

5e. TASK NUMBER
RR

5f. WORK UNIT NUMBER
A1

7. PERFORMING ORGANIZATION NAME(S) AND ADDRESS(ES)
Air Force Research Laboratory /VSBXT
29 Randolph Road
Hanscom AFB, MA 01731-3010

8. PERFORMING ORGANIZATION REPORT NUMBER
AFRL-VS-HA-TR-2007-1089

9. SPONSORING/MONITORING AGENCY NAME(S) AND ADDRESS(ES)

10. SPONSOR/MONITOR'S ACRONYM(S)
AFRL/VSBXT

11. SPONSOR/MONITOR'S REPORT NUMBER(S)

12. DISTRIBUTION/AVAILABILITY STATEMENT
Approved for Public Release; distribution unlimited.

13. SUPPLEMENTARY NOTES
Reprinted from Proceedings, 45th AIAA Aerospace Sciences Meeting and exhibit, 8-11 January 2007. Reno, NV. © 2007, AIAA
* Science Applications International Corp., San Diego, CA **NASA Marshall Space Flight Center, Huntsville, AL

14. ABSTRACT
Nascap-2k is a three-dimensional computer code that models interactions between spacecraft and plasma environments in low-Earth, auroral, geosynchronous, and interplanetary orbits. Previously, we reported on the accuracy of Nascap-2k's charging and current collections calculations by comparing computed currents and potentials with analytic results, and by comparing *Nascap-2k* results with published calculations using the earlier lower resolution codes, NASCAP/GEO, NASCAP/LEO, and POLAR. Here we examine the accuracy and limitations of two new capabilities of *Nascap-2k*: modeling of plasma plumes such as generated by electric thrusters and enhanced PIC computational capabilities. Nascap-2k models one or more ion engine plumes in full three-dimensional geometry, including plume-plume plume-spacecraft interactions. The primary thruster beam, parameters describing the neutral efflux, and the initial charge-exchange plume are imported from a *PlumeTool* generated file. *Nascap-2k* generates and tracks charge-exchange ions to obtain plasma densities and calculates potentials consistent with plasma densities and object surfaces. Nascap-2k's PIC capability has been expanded to include boundary injection, particle splitting, and substep charge deposition. We use calculations for simple geometries to explore the accuracy and limitations of these capabilities.

15. SUBJECT TERMS
Spacecraft charging, Plasma Simulation, Nascap-2k

16. SECURITY CLASSIFICATION OF: a. REPORT	b. ABSTRACT	c. THIS PAGE	17. LIMITATION OF ABSTRACT	18. NUMBER OF PAGES	19a. NAME OF RESPONSIBLE PERSON
UNCL	UNCL	UNCL			D.L. Cooke
					19B. TELEPHONE NUMBER *(Include area code)*

Nascap-2k Spacecraft-Plasma Environment Interactions Modeling: New Capabilities and Verification

V. A. Davis[*] and M. J. Mandell[†]
Science Applications International Corporation, San Diego, CA, 92121.

D. L. Cooke[‡]
Air Force Research Laboratory/VSBX, Hanscom Air Force Base, MA, 01731

and

D. C. Ferguson[§]
NASA Marshall Space Flight Center, Huntsville, AL, 35812

Nascap-2k **is a three-dimensional computer code that models interactions between spacecraft and plasma environments in low-Earth, geosynchronous, auroral, and interplanetary orbits. The code builds on physical principles, mathematical algorithms, and user experience developed over three decades of spacecraft charging research.** ***Nascap-2k*** **has improved numeric techniques, a modern user interface, and a simple, interactive satellite surface definition module (*****Object ToolKit*****).**

Capabilities include surface charging in geosynchronous and interplanetary orbits, sheath and wake structure and current collection in low-Earth orbits, and auroral charging. External potential structure and particle trajectories are computed using a finite element method on a nested grid structure and may be visualized within the ***Nascap-2k*** **interface. Space charge can be treated either analytically, self-consistently with particle trajectories, or consistent with imported plume densities. Particle-in-cell (PIC) capabilities are available to study dynamic plasma effects.**

Previously, we reported on the accuracy of ***Nascap-2k's*** **charging and current collection calculations by comparing computed currents and potentials with analytic results, and by comparing** ***Nascap-2k*** **results with published calculations using the earlier lower resolution codes, NASCAP/GEO, NASCAP/LEO, and POLAR. Here we examine the accuracy and limitations of two new capabilities of** ***Nascap-2k:*** **modeling of plasma plumes such as generated by electric thrusters and enhanced PIC computational capabilities.**

Nascap-2k **models one or more ion engine plumes in full three-dimensional geometry, including plume-plume and plume-spacecraft interactions. The primary thruster beam, parameters describing the neutral efflux, and the initial charge-exchange plume are imported from a** ***PlumeTool*****-generated file.** ***Nascap-2k*** **generates and tracks charge-exchange ions to obtain plasma densities and calculates potentials consistent with plasma densities and object surfaces.**

Nascap-2k**'s PIC capability has been expanded to include boundary injection, particle splitting, and substep charge deposition. The boundary injection replaces collected particles in long running calculations. The particle splitting allows for modeling the effects of the thermal distribution of velocities, as well as accommodating particle weight to variable grid cell volume. The substep charge deposition makes possible calculations in which two effects have significantly different timescales. We use calculations for simple geometries to explore the accuracy and limitations of these capabilities.**

[*] Sr. Staff Scientist, 10260 Campus Point Dr., M/S A1A, AIAA Member.
[†] Sr. Staff Scientist, 10260 Campus Point Dr., M/S A1A, AIAA Member.
[‡] Research Physicist, Space Vehicles Directorate, AIAA Member.
[§] Lead, Constellation Environments Test Integration Group, EM50, AIAA Senior Member.

I. Introduction

Designers of spacecraft for government, commercial, and research purposes require advanced modeling capabilities to guide the design of satellites that can survive and operate properly in the natural and induced environment. Computer modeling of flight experiments (including SCATHA, the SPEAR[1,2] series, and CHAWS[3]) has reliably predicted both steady-state and dynamic interactions between high-voltage spacecraft and the ambient plasma. Computer modeling has also been applied to inherently dynamic problems, such as those involving three-dimensional space charge sheath formation, current flow in the quasi-neutral presheath, breakdown phenomena, plasma kinetics, ionization processes, and the effect of unsteady processes on spacecraft charging.

Nascap-2k is being developed by Science Applications International Corporation (SAIC) to address this need. The development has been sponsored jointly by the Air Force Research Laboratory at Hanscom AFB and by NASA's Space Environments and Effects (SEE) Program at Marshall Space Flight Center. The current release is Version 3.1 and Version 3.2 is expected to be released before the end of 2007.

Nascap-2k is a widely used interactive toolkit for studying plasma interactions with realistic spacecraft in three dimensions. It can model interactions that occur in tenuous (*e.g.*, GEO orbit or interplanetary missions) and in dense (*e.g.*, LEO orbit) plasma environments. It incorporates the physics and numeric techniques developed over the last thirty years to address these interactions.

Nascap-2k has primarily been used to model spacecraft surface charging in tenuous plasmas, such as at geosynchronous orbit, and current collection from dense plasmas, such as in low-earth orbit. Validation of these capabilities has been addressed in a previous publication.[4] The code can also be used to examine particle trajectories, wake structure, and charging in dense plasmas. Recently two capabilities have been significantly enhanced. The inclusion of ion densities from plasma sources (such as thruster plumes) in the computation of potentials in space has been enhanced by the direct input of the ion plume and the self-consistent calculation of charge exchange. The particle-in-cell (PIC) capabilities have been enhanced to make PIC calculations more flexible, robust, and faster.

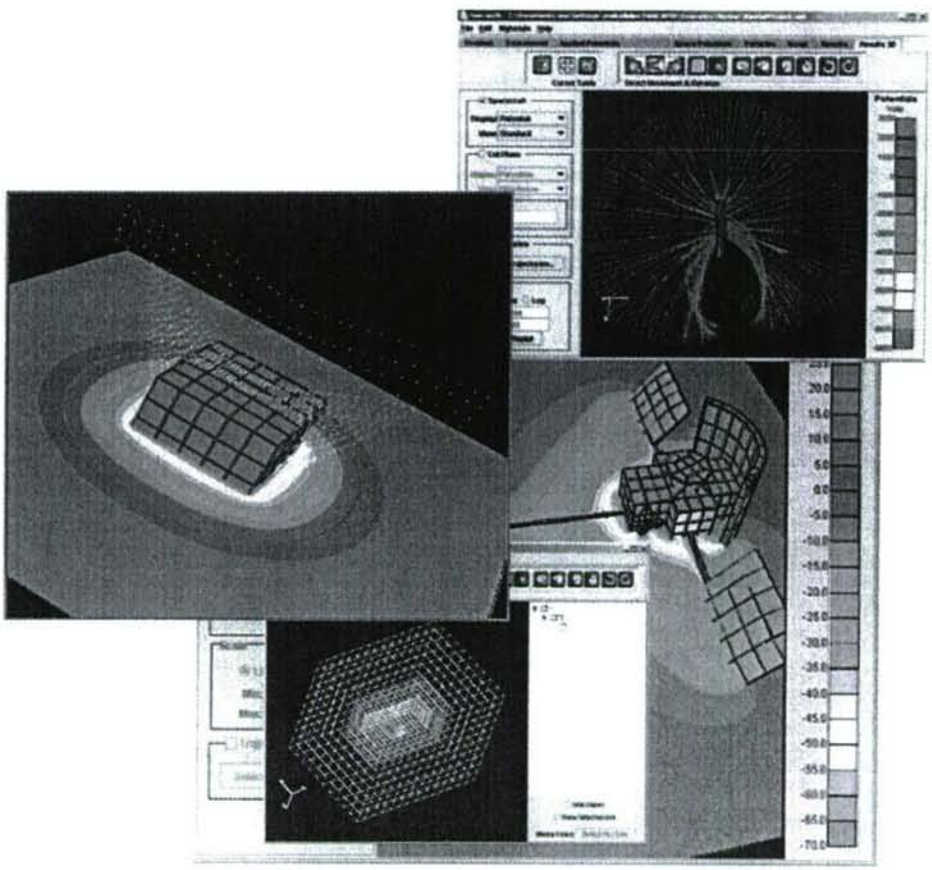

Figure 1. Views of *Nascap-2k* user interface.

II. *Nascap-2k*

Nascap-2k[5, 6, 7, 8 9] is a three-dimensional spacecraft plasma environment interactions computer code that simluates a wide variety of plasma phenomena. These include spacecraft charging in geosynchronous, interplanetary, auroral, and low-Earth-orbit plasmas, volume potentials, particle trajectories, and resulting variations in plasma density.

Nascap-2k is targeted to spacecraft design engineers, spacecraft charging researchers, and aerospace engineering students. The graphical user interface is designed to help less experienced users easily solve moderately complex plasma interactions problems while allowing the expert user to tackle questions that have not been previously contemplated.

The core capabilities of *Nascap-2k* are the following:

1. Define spacecraft surfaces and geometry and the structure of the computational space surrounding the spacecraft;
2. Solve for time-dependent potentials on spacecraft surfaces;
3. Solve the electrostatic potential about the object, with flexible boundary conditions on the object and with space-charge computed either fully by particles, fully analytically, or in a hybrid manner;
4. Generate and track electrons and ions, represented as macroparticles, including computing the resulting surface and volume, current and charge densities;
5. View surface potentials, space potentials, particle trajectories, and time-dependent potentials and currents.

The earliest and most common application of *Nascap-2k* is to study charging of spacecraft in geostationary orbit. *Nascap-2k* is designed to make this type of analysis particularly easy. *Nascap-2k* calculates surface potentials and electric fields using the Boundary Element Method (BEM),[10] thus a simple charging calculation does not require a spatial grid. *Nascap-2k* contains a selection of predefined Maxwellian, Double Maxwellian, and auroral plasma environments, which are readily modified to create custom environments. Other aspects of the environment include the magnetic field, the sun direction, and the sun intensity.

To solve for the electrostatic potential about the object, *Nascap-2k* uses a high-order finite element representation of the electrostatic potential that assures that electric fields are strictly continuous throughout space. The electrostatic potential solver[11] uses a conjugate gradient technique to solve for the potentials and fields on the spacecraft surface and through the surrounding space. Several analytic and numerical space charge density models are available, including Laplacian, Linear, Non-linear, Frozen Ions, Full Trajectory Ions, Hybrid PIC (appropriate to the several microsecond timescale response to a negative pulse), and Full PIC.

Particle tracking is used to study sheath currents, to study detector response, to generate steady-state charge densities, or to generate space charge evolution for dynamic calculations. *Nascap-2k* generates macroparticles (each of which represents a collection of particles) either at a "sheath boundary", the problem boundary, or throughout all space. Alternatively, particles can be initialized with a user-generated file. Particles are tracked for a specified amount of time, with the timestep automatically subdivided at each step of each particle to maintain accuracy. The current to each surface element of the spacecraft is recorded for further processing. The charge or current density created by the particles can be saved for use in solving for volume potentials.

III. Plumes in *Nascap-2k*

A recent enhancement made to *Nascap-2k* is enhancement of the ability to specify ion densities due to an ion source (ion thruster or plasma contactor, for example) and use them in the computation of potentials in space. Potentials due to plasma sources and object surfaces are needed to compute contaminant trajectories. This capability can be used to study the influence of spacecraft surfaces on engine plumes and interactions between plumes.

Nascap-2k's plume capabilities are intended to complement those of the *EPIC* (Electric Propulsion Interactions Code) computer code[12] which, like *Nascap-2k*, was developed by SAIC for NASA's SEE program. *EPIC* is a fast-running code that models plumes, places plumes on spacecraft, displays plume densities in space, and calculates plume fluxes to spacecraft surfaces and resultant surface effects (*e.g.*, sputtering). It is easy to modify parameters in *EPIC*, as well as to account for orbital configuration changes (*e.g.*, rotation of solar arrays). However, *EPIC* does not calculate potentials in space, and thus cannot account for the effects of surface potentials and surface sheaths, interactions between plumes, or self-consistent flow of charge exchange ions around obstacles, all of which are intended subjects for study with *Nascap-2k*.

A two-dimensional (RZ) map of the ion density due to a plasma source can be imported directly into *Nascap-2k*. The locations and directions of all instances of the plume are specified. *Nascap-2k* then solves a nonlinear Poisson equation for space potentials using the surface potentials as boundary conditions. The charge density consists of the known ion density from the plume specification plus a barometric electron density:

$$\frac{\rho}{\varepsilon_0} = \frac{\rho_{ion}}{\varepsilon_0}\left(1 - \exp\left(\left(\phi - \phi_b\right)/\theta\right)\right)$$
$$\phi_b = \theta \ln\left(\frac{\rho_{ion}}{en}\right) \tag{1}$$

where θ and n are the plume electron temperature and reference density respectively, ρ is the total charge density to be used in Poisson's equation, and ρ_{ion} is the known ion density. In addition to the specification of the ion density from an external plume map, charge exchange ions, such as those generated in a ion thruster plume, can be generated and tracked within *Nascap-2k* to achieve a self-consistent solution[13].

This capability was used to analyze plume interactions, charge exchange ion density and flow, and surface impingement in NEXT multiple thruster tests[14] conducted at NASA Glenn Research Center during December 2005. The test configuration includes three active NEXT thrusters plus a dummy thruster in the fourth position, as well as a full complement of diagnostic probes. The objective of the test was to identify and quantify the beneficial and deleterious interactions between the engines, their plumes, and their controlling electronics.

Figure 2 shows the potentials of the superposed plumes of the three active thrusters on a plane through the center of two of the thrusters. This is used as an initial condition for the calculations, and also serves as a point of comparison to note thruster interaction effects. Except immediately adjacent to biased surfaces, the potentials are barometric, *i.e.*, approximately logarithmic with the ion density.

Figure 3 shows the potentials on the same plane as in Figure 2, after calculating the self-consistent potentials by generating and tracking charge exchange ions in the potentials and recomputing potentials until a self-consistent solution is reached. Differences of note between the self-consistent potentials (Figure 3) and the superposed potentials (Figure 2) include the following:

1. Treatment of the blockage of ions by the thrusters and backing plate. The blockage of ions by the thrusters and backing plate is not included when the plumes were initially generated and superposed, resulting in substantial charge exchange ion density behind the blocking plate. The self-consistent calculation shows low ion density behind the plate and a sensible potential and density structure at the edge of the plate.
2. A charge exchange ion stagnation region occurs about one thruster diameter above the midpoint between the two thrusters. In the superposed plume structure, charge exchange ions are accelerated laterally out of one plume and pass unphysically through the neighboring plume, whereas in the self-consistent structure ions are blocked by the positive potentials of the neighboring plume.
3. The downstream potentials and densities are higher in the self-consistent plume than in the superposed plume, probably because of inhibition of lateral motion by neighboring plumes.

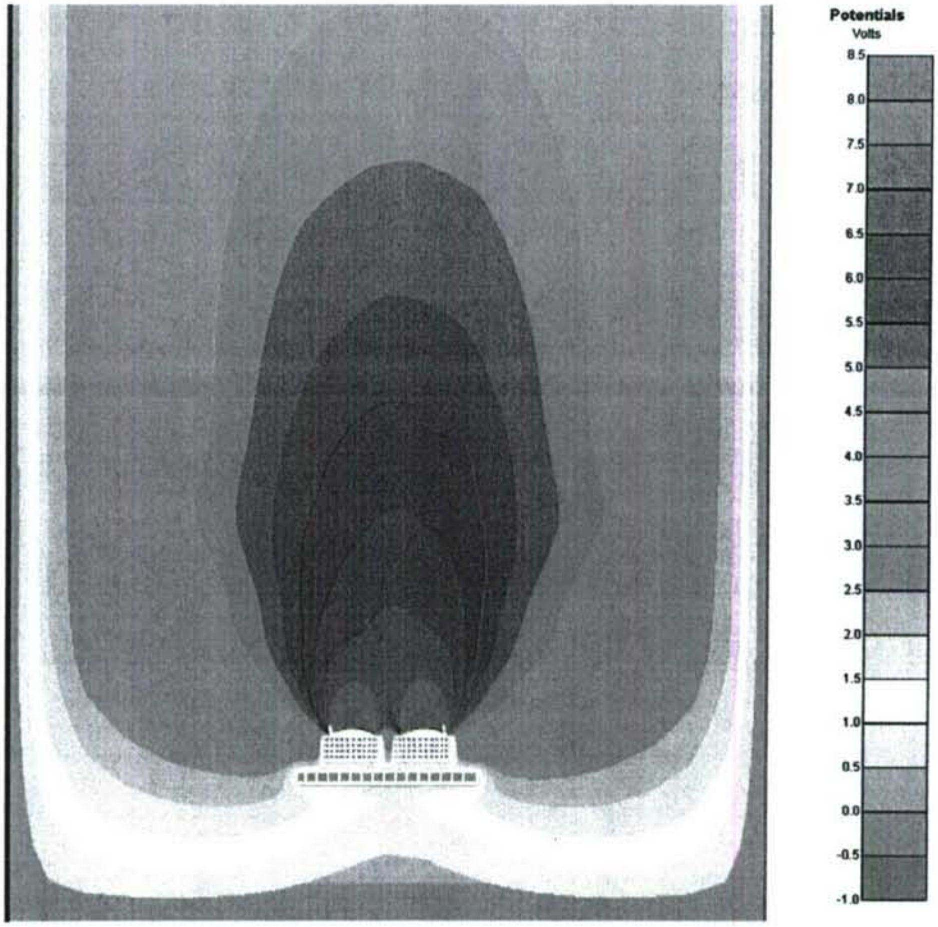

Figure 2. Potentials in the plumes of the thruster array with the total density a superposition of the individual plumes, used as initial condition for the calculation. (Half of chamber length is shown.) Contours are in a plane through the center of two active thrusters. Potential and density is biased toward the right due to the dummy thruster at the left rear.

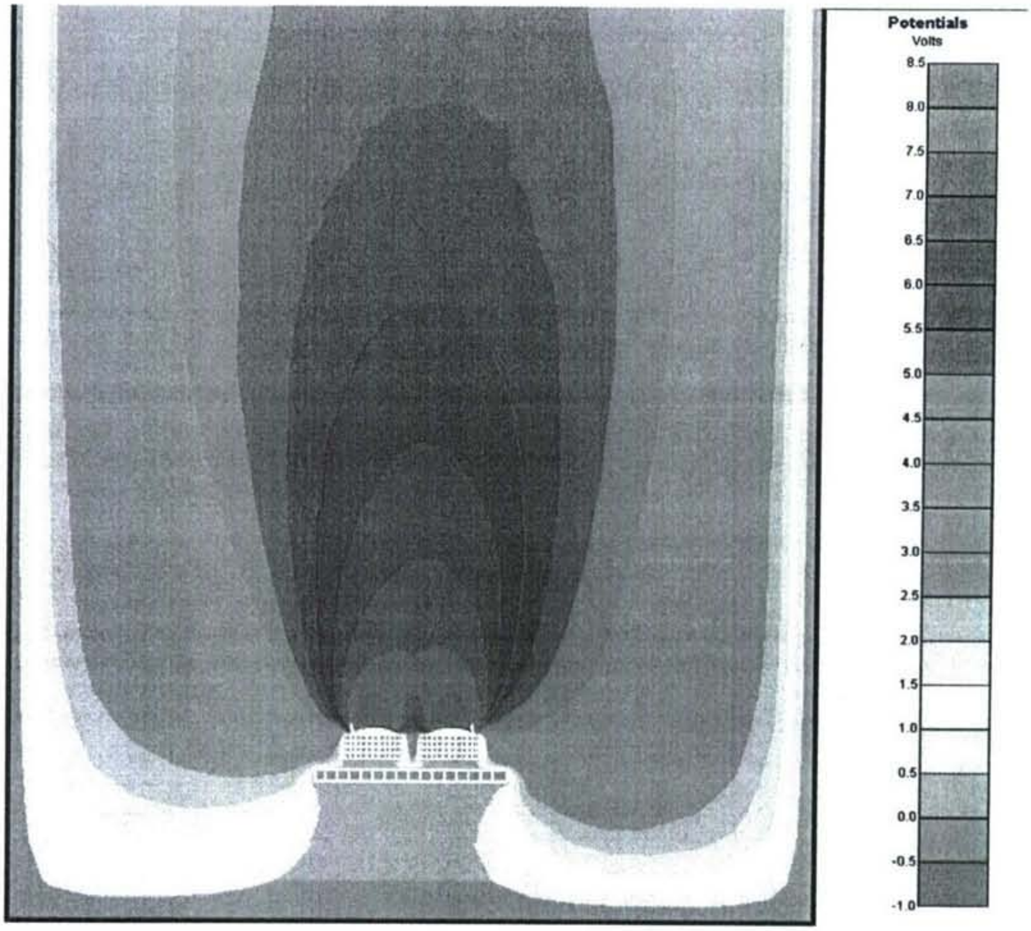

Figure 3. Self-consistent potentials in the plumes of the thruster array. (Half of chamber length is shown.) Contours are in a plane through the center of two active thrusters. Potential and density is biased toward the right due to the dummy thruster at the left rear.

IV. Particle in Cell Calculations

Nascap-2k has primarily been used to model quasi-static phenomena. However, there are a large number of physical processes of interest whose timescales require a dynamic approach, such as a particle-in-cell (PIC) technique. Examples of such processes are breakdown phenomena, plasma kinetics, and sheath structure about surfaces with potentials that change on a timescale comparable to the time it takes an ion to cross the sheath. PIC techniques can also be used to address problems in which analytic representations of the environmental currents are inadequate, such as in a spacecraft wake or in a cavity. A PIC technique, in which the ion space charge density is computed from macroparticles tracked from the boundary of the computational space until they are collected or exit the computation space, was successfully used to model the CHAWS experiment. In addition, PIC techniques can be useful when developing analytic models. In order to facilitate these modeling techniques, the ability to perform various types of PIC calculations was built into *Nascap-2k*. Recently, additional numeric techniques have been added to make two types of PIC calculations more flexible, robust, and faster—Hybrid PIC and full PIC. In a Hybrid PIC calculation, the problem is initialized by creating ion macroparticles throughout the grid to represent a constant particle density. The ion macroparticles are tracked for one timestep and then volume potentials are computed using the resulting ion density and a barometric electron density. The process is repeated for the time period of interest. In a full PIC calculation, both electron and ion macroparticles are tracked and volume potentials are computed using the resulting plasma density. The user interface was also revised to make such calculations simpler to specify and to analyze.

Of primary interest is VLF (about 1 to 20 kHz) antennas in the upper ionosphere. Plasma waves from VLF antennas with such frequencies are thought to interact with MeV radiation belt electrons. Such an antenna would be a rod several inches in diameter and many meters long and, due to the ease of electron collection by positive objects, would be nearly always at negative potential relative to the ambient ionosphere. Because the frequencies of interest are comparable to the ion plasma frequency, the sheath structure will be at some intermediate state between the "ion matrix" or "frozen ion" limit (which assumes the ions are stationary and contribute ambient ion density to the space charge) and the equilibrium space charge limit (in which the ions assume a steady-state space charge limited distribution of charge and current). Thus, calculation of the sheath structure and of the ion collection by the antenna requires dynamic (PIC) treatment, at least for the ions. *Nascap-2k* can be used to perform all four simulations of interest: (1) equilibrium space charge sheath; (2) "frozen ion" sheath; (3) dynamic PIC ions with fluid (Boltzmann or barometric) electrons (Hybrid PIC); (4) dynamic PIC ions and electrons (Full PIC).

Two of these recent enhancements to *Nascap-2k*'s PIC capabilities are the injection of macroparticles from the boundary during a calculation and the splitting of the macroparticles.

In order to replace macroparticles that are collected by the probe or escape from the grid, it is necessary to periodically inject macroparticles from the boundary. This allows for the calculation of current for longer time periods. In hybrid PIC calculations without boundary injection, the low field region near the boundary of the problem develops a significant negative potential due to ion depletion. Boundary injection keeps these potentials near zero by replenishing the ions that have been collected or escaped.

Particle injection is implemented with an injection point at each quarter-boundary-surface-element. The injected particle has charge equal to the plasma thermal current times the area times the time interval, and velocity equal to $\sqrt{\frac{2eT}{\pi m}}$, so that it represents the inbound half of the plasma density. When the spacecraft is moving through the plasma this algorithm is modified to account for the motion. The current and velocity are computed in such a way that the density contribution of the injected particles varies from half the ion density for a stationary object to the full ion density for a high mach number object.

Closely connected with boundary injection is macroparticle splitting. There are two major reasons for splitting macroparticles: one physical and one numeric. Even at moderate potentials, thermal effects can reduce collected currents. Some particles near the sheath edge have enough thermal velocity perpendicular to the electric field that angular momentum conservation prohibits collection. Particle splitting allows for a representation of the thermal distribution in the initial particle distribution and in particles injected from the boundary. From a numeric point of view, particle splitting can be used to keep the particle weight appropriate to the grid size and to help maintain the smoothness of the distribution. A large particle that originated in an outer grid is split so that it becomes distributed over several volume elements in an inner grid.

Macroparticles may be split when they enter a more finely resolved region or when they are created either at the boundary or throughout the volume at problem initialization. The algorithm used is as follows:

1. Particles are split in velocity space only. Because high-field regions are often of interest, spatial splitting would raise problems with energy conservation.
2. Each particle carries a temperature, which is treated as isotropic. The fission products carry half the temperature of the original particle, while the remaining thermal energy appears as kinetic energy of the split particles. That each macroparticle has a temperature means that they can be split repeatedly in mid-flight, each time the particle enters a more finely resolved region.
3. For splitting purposes the Z-axis is defined to be along the direction of the particle velocity, the X-axis randomly chosen in the plane normal to Z, and the Y-axis mutually perpendicular.
4. Particles are split into two or three particles along each axis, except that a particle is not split along the Z-direction if the kinetic energy exceeds the thermal energy. Not splitting along Z helps avoid particle proliferation, but makes an error by not preserving the original particle temperature along Z. Eight, nine, or twenty-seven new particles result.
5. Particle velocity is assumed to be acquired by acceleration rather than actual drift (i.e., spacecraft velocity). If there is actual drift, then the drift velocity is removed before splitting the particle and added back after.
6. If the particle is split by two along the X or Y axis, the new velocity is $\pm 0.707\sqrt{\mathrm{T/m}}$. Along the Z axis the velocity increment is calculated as if the temperature were $\mathrm{T} - 2\mathrm{mu}_0^2\left(\sqrt{1+\frac{\mathrm{T}}{\mathrm{mu}_0^2}}-1\right)$.

7. If the particle is split by three along the X or Y axis, there is a zero-velocity central particle and two "probe" particles with velocity is $\pm 0.866\sqrt{T/m}$. Along the Z axis the velocity increment is calculated as if the temperature were $T - 2mu_0^2\left(\sqrt{1+\frac{T}{mu_0^2}}-1\right)$.
8. The new particles have the same properties as the original particle except for velocity, weight (charge), and temperature.

We use *Nascap-2k* to compute the current collected by a 10 cm radius, -100 V sphere in a 10^{10} m^{-3}, 1 eV, H^+ plasma. The sphere, represented by the 32 surface quasisphere shown in Figure 4, is embedded in a 2.4 m cubic grid. The plasma density is computed using the Hybrid PIC charge density model with timesteps of 5 x 10^{-7} s. The collection of ions by the probe and the loss of ions out the sides are monitored, and the final potential and particle configurations are inspected.

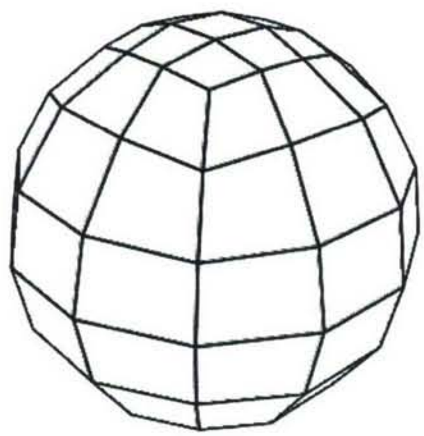

Figure 4. Sphere object used in example.

The sphere is a useful test case not only because the equilibrium current can be analytically computed, but because the symmetry provides a good test of the ability of the splitting to properly represent the angular momentum barrier. An analytic formulation gives the equilibrium sheath radius of 73 cm for a collected current of 41 microamperes. Presheath enhancement[15] gives another factor of 1.45 for 59 microamperes. Presheath enhancement is the focusing of current outside the sheath. The PIC approach automatically includes the presheath enhancement. The current leaving the grid is the surface area of the grid times the one-sided plasma thermal current for a total of 216 microamperes.

Figure 5 compares the collected, leaving, and injected current for a calculation with particle splitting and boundary injection and a calculation with neither. The collected current rapidly rises to a sustained value of about 60 microamperes. Without splitting the current fluctuates widely. With no splitting, there is no current leaving the grid as the electric field points toward the grid center and there is no thermal motion. With splitting and injection, the escaping and injected currents are much larger than the collected current, averaging 160 to 170 microamperes. The injected current is, on average, slightly greater than the escaping current, and far less than the sum of the collected and escaping currents.

Figure 6 and Figure 7 show the potential contours for the two calculations after 50 microseconds. The potentials are spherical. While the potentials with no splitting or boundary injection look smoother, after 50 microseconds they are extending further from the sphere as the total ion charge in the grid is depleted. The potential fluctuations in the case with splitting and boundary injection are all well under the plasma temperature of 1 eV.

For comparison, Figure 8 and Figure 5 show results for the case with splitting but no particle injection. In this case, between the sheath edge and the grid boundary, the potential is more negative than -0.3 volts. This is because the ion population is depleted due to both collection of ions by the probe and by escape of ions through the grid boundary due to their thermal motion. Significant potential drop can be caused by a relatively small depletion, so that at 50 microseconds the collected current is not significantly reduced.

These improvements come at a considerable cost in computing time and disk space. From an initial particle count of 0.3 million for the case with no splitting and no injection, the particle count decreases to 0.1 million at 50 microseconds; while the run with particle splitting and boundary injection starts at 2.4 million particles and increases to 8.4 million at 50 microseconds.

Figure 9 shows a quadrant of particles after nine microseconds. The particles are initially unsplit, and the ions are split into nine or twenty-seven particles on entering a finer grid. In Figure 9 ions can be seen entering Grid 2 from Grid 1 at the top and right. Because these ions are moving slowly, they are split both along and normal to their motion direction. By this time all ions originating in Grid 3 have been "eaten" by the sphere, so that the cloud of ions currently in Grid 3 have entered from Grid 2 and been split. Those that entered most recently were already drifting significantly when they were split, and were thus split only normal to their direction of motion.

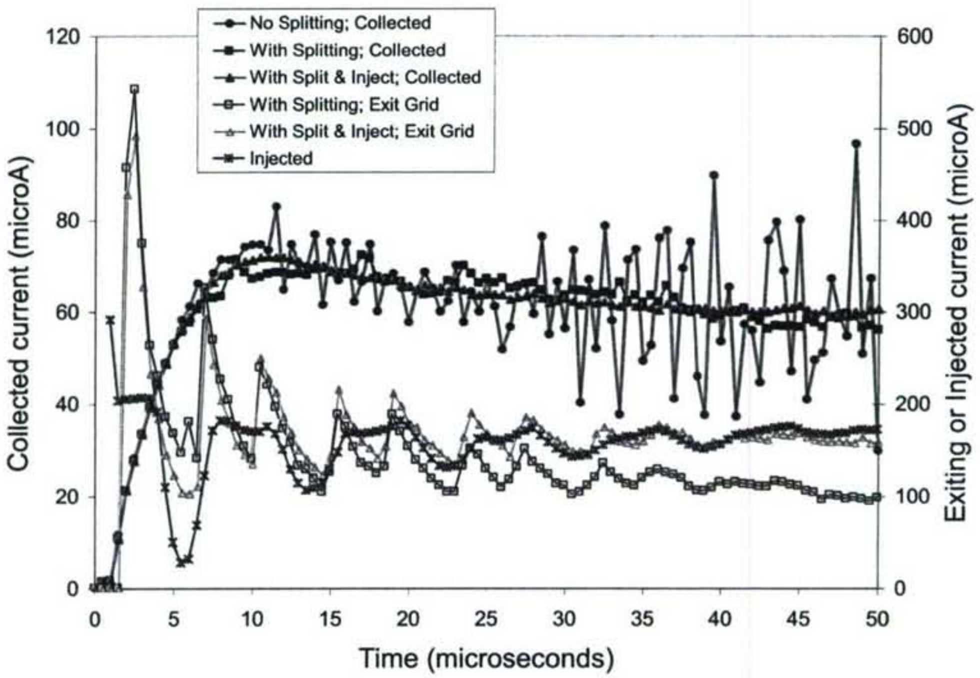

Figure 5. Collected current (left scale), escaping current (right scale), and injected current (right scale) running problem with boundary injection.

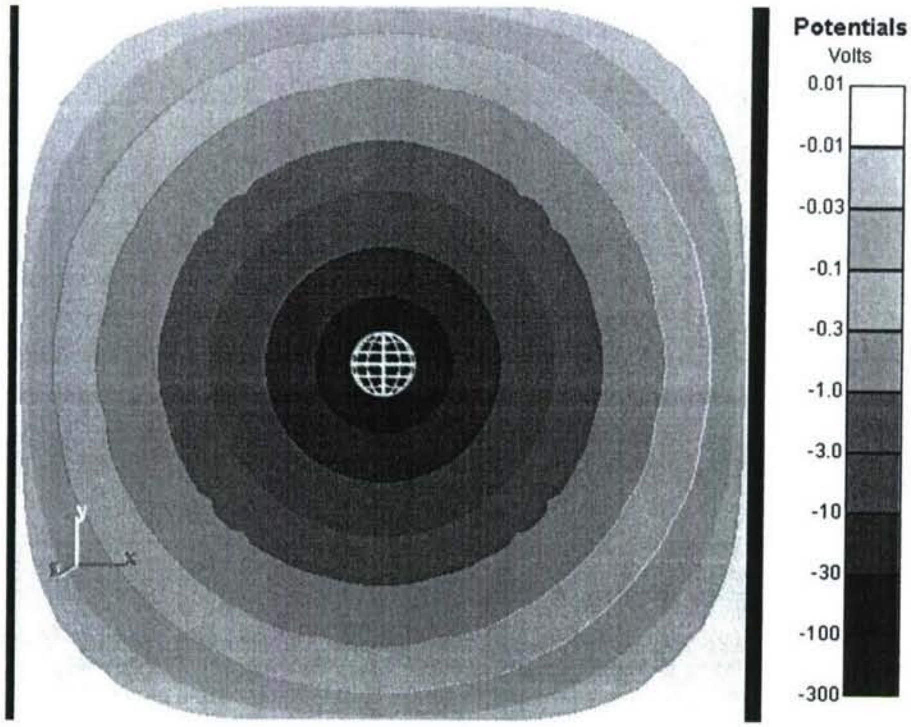

Figure 6. Potential contours after 50 microseconds for Hybrid PIC calculation with no particle splitting and no boundary injection.

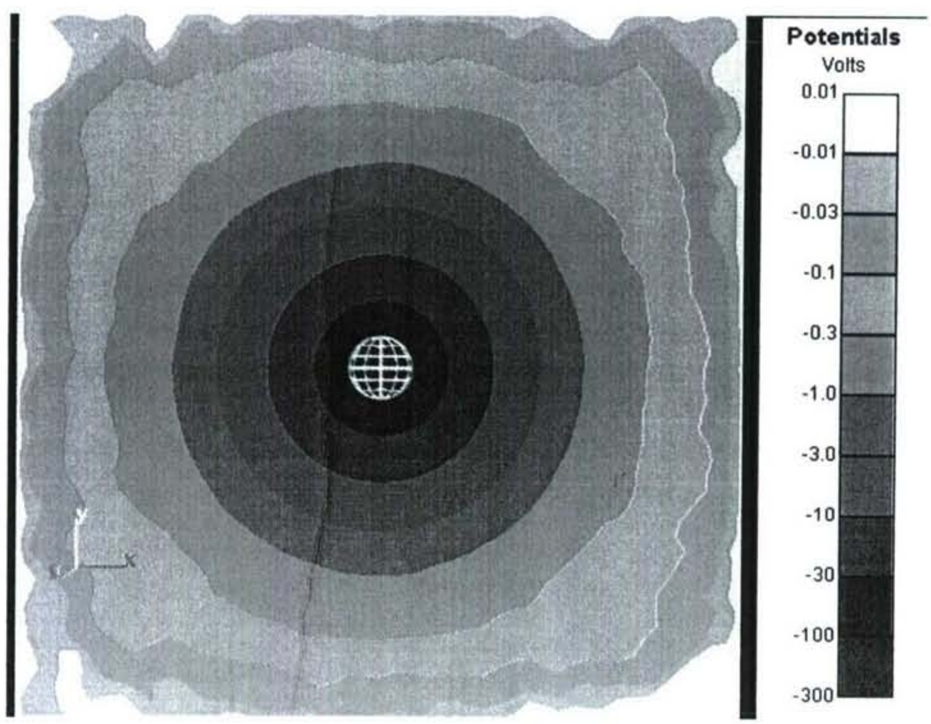

Figure 7. Potential contours after 50 microseconds for Hybrid PIC calculation with particle splitting and boundary injection.

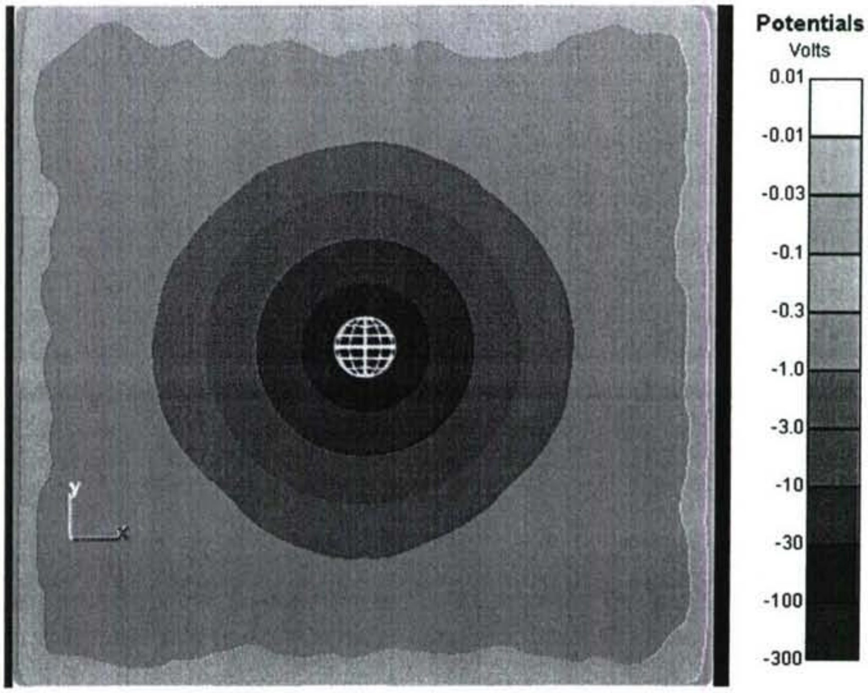

Figure 8. Potential contours after 50 microseconds for Hybrid PIC calculation with particles split upon creation and upon entering grid with finer resolution, but no boundary injection.

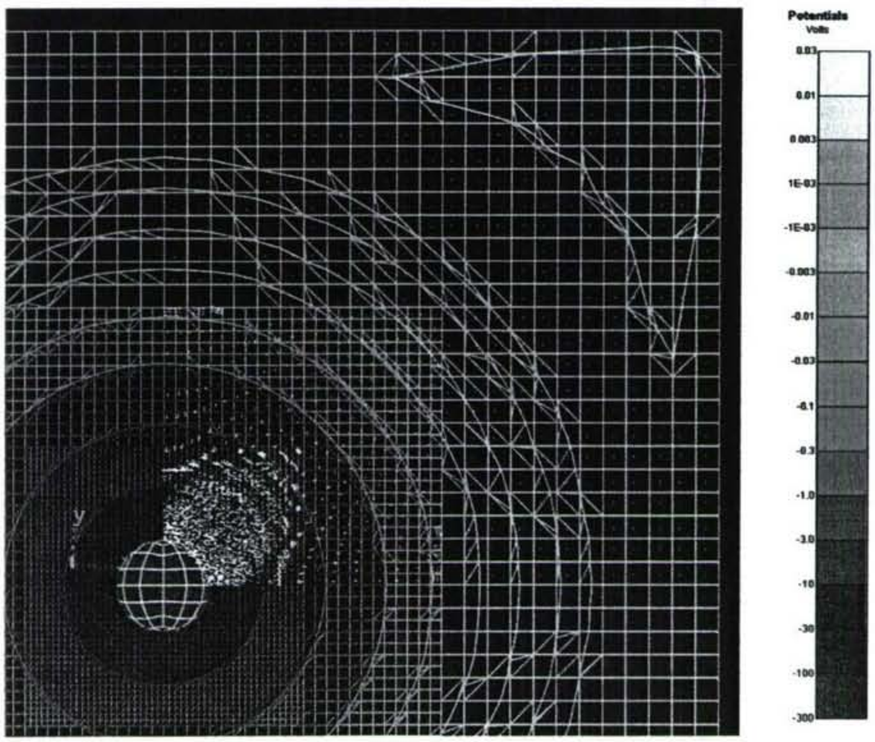

Figure 9. Particle positions after nine microseconds when particles are split on entering a more finely resolved grid.

The thermal distribution of the ions plays an important role in the formation of the wake structure. To illustrate this, we examine the wake structure with and without splitting. Figure 10 shows a hybrid PIC calculation (with no particle splitting) of O+ flow past an uncharged sphere moving at LEO velocity in the (1,1,0) direction. Clearly seen are the negative potentials in the object wake and the boundary between the injected particles (diagonal pattern) and the original particles (square pattern). Potential fluctuations on the order of 0.05 volts are seen in the first subdivided grid where it is populated by outer grid ions. Figure 11 shows a similar calculation, now with the sphere at -100 V. After 136 microseconds ions are focused in the wake sufficiently strongly to create positive potentials near the ram energy. (Note that this rather striking result is probably associated with the object size being comparable to the plasma debye length.)

Figure 12 shows the charged sphere calculation, now with particles split on entering a refined grid. While the general character of the result is the same, the potentials are much smoother and now show compression of the sheath on the ram side. Figure 13 shows the current to the sphere. After an early peak to nearly 16 microamperes, the current settles down to a value of less than 7 microamperes, comfortably less than the orbit-limited value of 8 microamperes. Of course, this improved fidelity comes at a price, with a final particle count in excess of two million in Figure 12, versus. under 0.4 million in Figure 11.

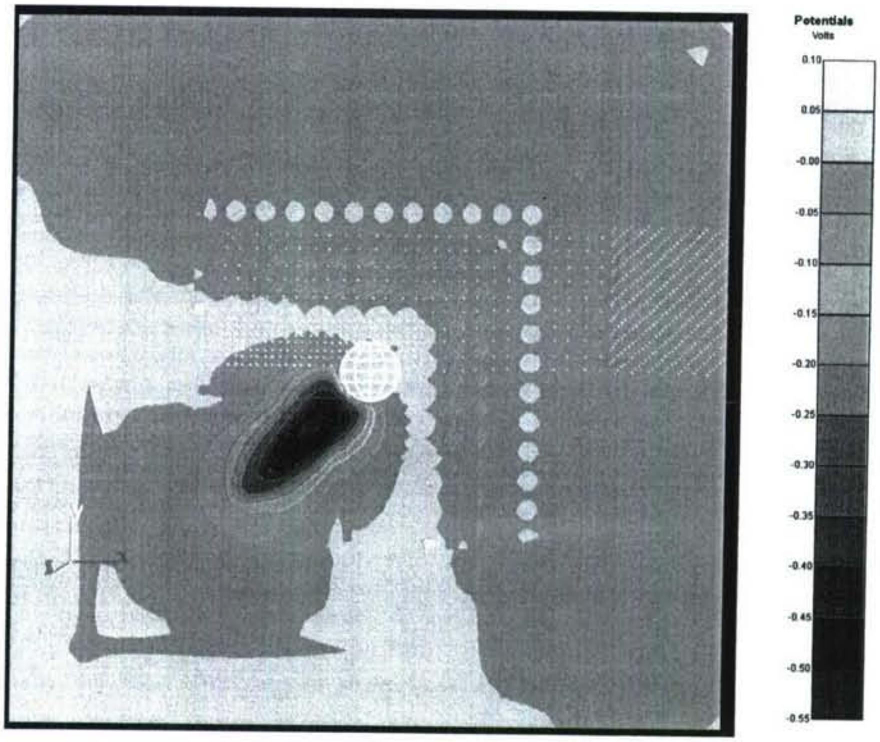

Figure 10. Potentials and ion (O^+) macroparticles after 80 microseconds for an uncharged sphere moving in the (1,1,0) direction. (No splitting of macroparticles.)

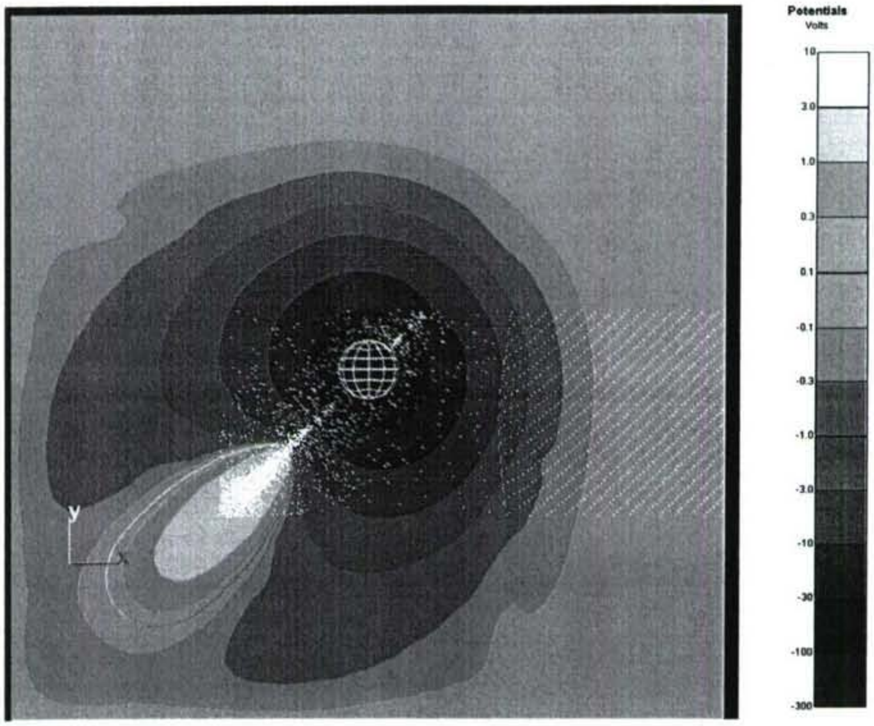

Figure 11. Potentials and ion (O^+) macroparticles after 136 microseconds for -100 V sphere moving in the (1,1,0) direction. (No splitting of macroparticles.)

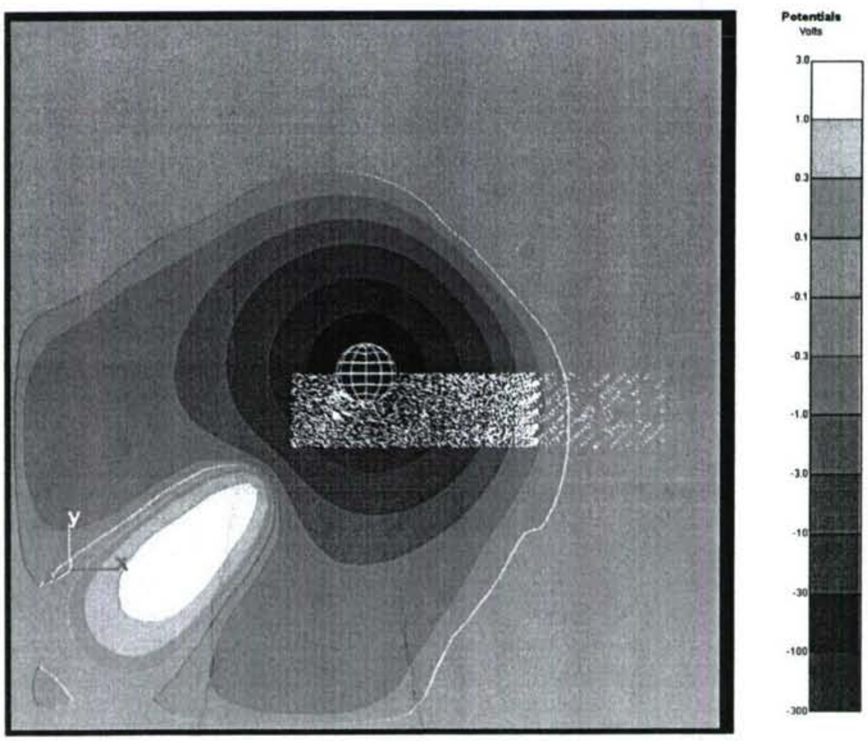

Figure 12. Potentials and ion (O^+) macroparticles after 160 microseconds for a sphere charged to -100 V moving in the (1,1,0) direction. Particles split on entering refined grid.

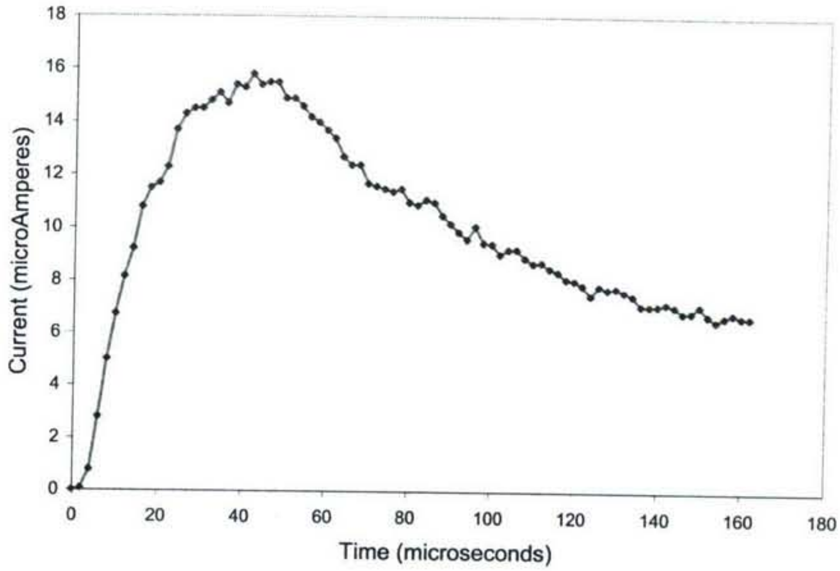

Figure 13. Current for sphere charged to -100 V moving in the (1,1,0) direction. Particles split on entering refined grid.

Another new capability is orbit averaging. Previously *Nascap-2k* could perform two kinds of particle in cell calculations. In one kind, used to model the CHAWS experiment, which involved current collection by a high potential in the wake region of a disk shaped spacecraft (WSF), macroparticles are created at the boundary of the computational space and are tracked until they either are collected by the object or leave the computational space. These macroparticles carry current and share the current times the sub-step time in each volume element each sub-step. After all the macroparticles are tracked, potentials are computed using the ion charge deposited by the tracked macroparticles. The full trajectory tracking is iterated with the potential solution until a self-consistent solution is found. Often mixing of the present and previous solutions is necessary to reach self-consistency. The other type of PIC calculation is the traditional approach discussed above, in which the macroparticles are only tracked for a single timestep and their entire charge is deposited on the computational nodes at the end of the timestep. This approach is needed for time-dependent phenomena.

Orbit averaging is a variation of the standard PIC approach in which a portion of the macroparticle's charge is deposited to the grid each substep. This approach is appropriate when the timescales of the phenomena of interest are long compared with the time it takes a particle to transit a volume element. The timestep can be appropriate to the phenomena of interest, while the substeps are such that the particles travel only a fraction of mesh unit. This approach can give a much smoother solution as seen in Figure 14. A variation will be appropriate for the tracking of electrons when the timestep is set by the ion transit time.

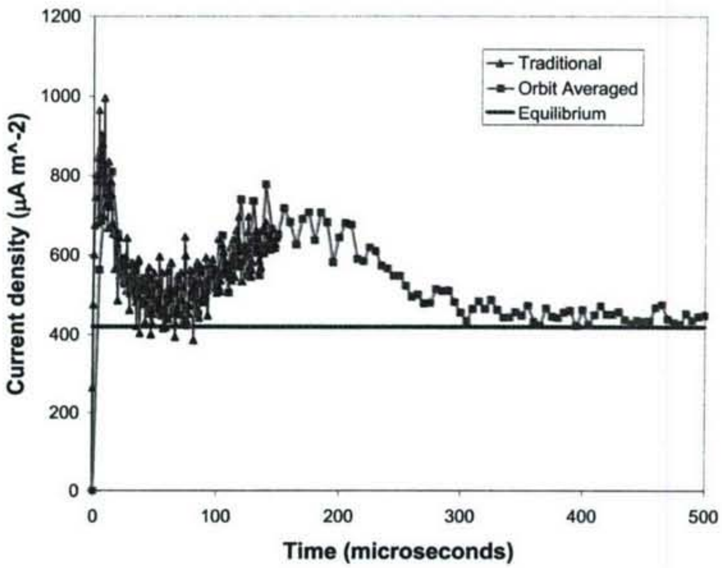

Figure 14. Current to sphere with standard PIC approach and with orbit averaging.

The final improvement we discuss is the ability to compute the change in surface potentials, charging, due to tracked ions from a Hybrid PIC or full PIC calculation. This capability makes it possible to calculate spacecraft floating potential and differential charging for cases where analytic approximations to plasma currents are not adequate, for example with a dynamic bias or a concave geometry.

When this technique is used, ions are tracked and the net surface current is the sum of the tracked ion current and an analytic electron current. The electron current is a function of the surface area, A, the electron thermal current, j_{th}, the surface potential, ϕ, and the plasma temperature, θ.

$$I = \begin{cases} Aj_{th} \exp(\phi/\theta) & \text{if } \phi \le 0 \\ Aj_{th}\left(1+\dfrac{\phi}{\theta}\right) & \text{if } \phi > 0 \end{cases} \tag{2}$$

We compare the analytic and numeric calculations of the discharge of a 0.1-m radius, -100 V sphere in a 10^{10} m^{-3}, 1 eV, hydrogen plasma. The *Nascap-2k* calculation is done using a 32 surface quasisphere shown in Figure 4. The plasma density is computed using the Hybrid PIC charge density model with timesteps of 5 x 10^{-7} s.

The change in potential of a sphere of radius r in vacuum due to an incident current I during a timestep of length τ is given by $\Delta\phi = \dfrac{I\tau}{C}$ where $C = 4\pi\varepsilon_0 r$. Figure 15 compares the potential computed by *Nascap-2k* with the potential computed from the capacitance of a sphere of radius 0.1 m and the tracked current. The figure also shows the potential computed for the capacitance of a sphere of radius 0.09285 m.

With the analytic electron current, the total current drops to zero as the potential becomes slightly positive, and the potential is held near zero by the incident electrons. The ion current remains at a fairly constant rate due to the inertia of the ions. Since the ion current is, on average, slightly less than the raw electron thermal current, the potential, on average, is slightly negative.

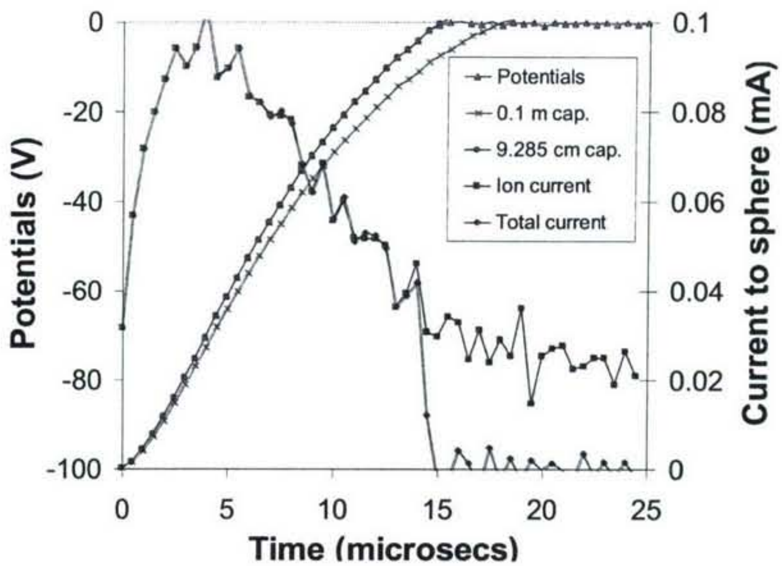

Figure 15. Current to sphere and resulting potentials for self-consistently computed discharge.

V. Conclusion

The recent enhancements of *Nascap-2k* will allow users to analyze a wider variety of spacecraft-plasma interactions. The improvements to the ability to specify ion densities due to an ion source and use them in the computation of potentials in space allows for modeling of thrusters plasmas. The new PIC capabilities will allow users to address fully dynamic problems in addition to quasistatic interactions for which it is already widely used.

The capabilities described here will be available in the next code release later this year. *Nascap-2k* is distributed through the SEE program web site, http://see.msfc.nasa.gov.

Acknowledgements

This paper was prepared with funding from the Air Force Research Laboratory.

References

[1] I. Katz, G.A. Jongeward, V.A. Davis, M.J. Mandell, R.A. Kuharski, J.R. Lilley, Jr., W.J. Raitt, D.L. Cooke, R.B. Torbert, G. Larson, and D. Rau, Structure of the Bipolar Plasma Sheath Generated by SPEAR I, *J. Geophys. Research* Vol. 94, A2, p. 1450, 1989.

[2] M.J. Mandell, G.A. Jongeward, D.L. Cooke, W.J. Raitt, "SPEAR 3 flight analysis: Grounding by neutral gas release and magnetic field effects on current distribution," *J. Geophys. Research* Vol. 101, A1, p. 439, 1998.

[3] V. A. Davis, M. J. Mandell, D. L. Cooke, L. Enloe, "High-Voltage Interactions in Plasma Wakes: Simulation and Flight Measurements from the Charge Hazards and Wake Studies (CHAWS) Experiment," *J. Geophys. Research* Vol. 104, 12445-12459, 1999.

[4] V. A. Davis, M. J. Mandell, B. M. Gardner, I. G. Mikellides, L. F. Neergaard, D. L. Cooke, J. Minor, "Validation of *Nascap-2k* Spacecraft-Environment Interactions Calculations," *8th Spacecraft Charging Technology Conference*, Huntsville, AL, October 2003.

[5] M.J.Mandell, I. Katz, J.M. Hilton, J. Minor, D.L. Cooke, *Nascap-2k*, A Spacecraft Charging Analyis Code for the 21st Century, AIAA Paper 2001-0957, *AIAA Aerospace Sciences Meeting & Exhibit, 39th, Reno, NV*, Jan. 2001.

[6] M.J. Mandell, I. Katz, D. Cooke, *Towards a more robust spacecraft charging algorithm*, AIAA Paper AIAA 99-0379, 1999.

[7] M.J. Mandell, V.A. Davis, B.M. Gardner, I.G. Mikellides, D.L. Cooke, J. Minor, *Nascap-2k*—An Overview, IEEE.

[8] V. A. Davis, L. F. Neergaard, M.J. Mandell, I. Katz, B.M. Gardner, J. M. Hilton, J. Minor, *Spacecraft Charging Calculations: Nascap-2k and SEE Interactive Spacecraft Charging Handbook*, AIAA Paper, AIAA 2002-0626, 2000.

[9] V. A. Davis, M. J. Mandell, B. M. Gardner, I. G. Mikellides, L. F. Neergaard, D. L. Cooke, J. Minor, "Validation of *Nascap-2k* Spacecraft-Environment Interactions Calculations," *8th Spacecraft Charging Technology Conference*, Huntsville, AL, October 2003.

[10] S. A. Brebbia, *Boundary Element Methods*, Springer Verlag, New York, 1981.

[11] M.J. Mandell, G.A. Jongeward, D.L. Cooke, W.J. Raitt, "SPEAR 3 flight analysis: Grounding by neutral gas release and magnetic field effects on current distribution," *J. Geophys. Research* Vol. 101, A1, p. 439, 1998.

[12] I.G. Mikellides, M. J. Mandell, R. A. Kuharski, V. A. Davis, B. M. Gardner, J. Minor, "The Electric Propulsion Interactions Code," *8th Spacecraft Charging Technology Conference*, Huntsville, AL, October 2003.

[13] M. J. Mandell, "NEXT Multi Ion Engine Test: Plume Modeling and Test Plans," 29th International Electric Propulsion Conference, Princeton University, 2005, paper IEPC-2005-285.

[14] M. J. Mandell, "NEXT Multi Ion Engine Test: Plume Modeling and Test Plans," 29th International Electric Propulsion Conference, Princeton University, 2005, paper IEPC-2005-285.

[15] M. J. M. Parrot, L. R. O. Story, L. W. Parker, J. G. Laframboise Theory of cylindrical langmuir probes in the limit of vanishing debye number, *Phys. Fluids, 25*, 2388, 1982.